

## Review of Industrial Engineering Letters

2014 Vol. 1, No. 2, pp. 1-20

ISSN(e): 2408-9427

ISSN(p): 2409-2169

DOI: 10.18488/journal.71/2014.1.2/71.2.55.66

© 2014 Conscientia Beam. All Rights Reserved.



# ESTIMATION OF COOLING RATE AND ITS EFFECT ON TEMPERATURE DEPENDENT PROPERTIES IN GTA WELDED HIGH CARBON STEEL JOINTS

J. Dutta<sup>1†</sup> --- Narendranath, S.<sup>2</sup>

<sup>1,2</sup>Department of Mechanical Engineering, National Institute of Technology Karnataka, Surathkal, Mangalore, India

## ABSTRACT

*An elaborate study has been conducted in this article to estimate the cooling rate of the Gas Tungsten arc (GTA) welded steel butt joints of grade AISI 1090. The temperature dependent thermal parameters has been investigated in connection with developed rate of cooling. Experiment has been carried out ffito determine the thermal cycle formed along the longitudinal direction from weld bead. Implementing experimental temperatures, Adams empirical cooling rate correlation has incorporated to analyze rate of cooling. A correlation has been suggested in this study, derived from thick plate temperature distribution model. To find out the heat loss from the joint, Vinokurov's empirical combined heat transfer coefficient has been utilized and with it has verified with conventional heat transfer coefficient based on convection and radiation. Cooling rate has been found out to be very rapid at  $z = 36\text{mm}$  to  $z = 108\text{mm}$  based on thick plate model and it has completely agreed with the variation of Adams correlation. At higher temperatures above  $800^\circ\text{C}$ , heat loss due to radiation completely dominates the convection and lower temperatures convection heat loss influences much than radiation. Heat loss due to convection and radiation fully justified with the results produced based on cooling rate and rapid cooling near the fusion boundary exists only for 5s-10s.*

**Keywords:** Rate of cooling, GTA welding, Heat loss, Temperature cycle, Thermal conductivity, Butt joint.

## Contribution/ Originality

The paper's primary contribution is finding the cooling rate and its effect on related thermal properties in Gas Tungsten Arc (GTA) welding of high carbon steel joints. Basically in present analysis, 0.9% C containing high carbon steel (AISI 1090) butt weld joint has been prepared and experimental temperature distribution has been analyzed. The effect of rapid temperature cycle formed and its dynamic effect on temperature dependent properties such as thermal conductivity, rate of cooling based on convection, radiation and evaporation has been studied. Cooling rate has

been estimated by 'Thick Plate Model', due to its close validation with experimental temperature cycle. This study reveals that all the temperature dependent properties are very randomly changing near the heat affected zone within the time range of 5s-10s. This article gives parametric study of effect of cooling rate and temperature dependent parameters developed in GTA welding of butt joints.

## 1. INTRODUCTION

To design the weld joints for the application based on naval and shipbuilding industries, automobile industries, nuclear reactor components, estimation of cooling rate plays an important role to judge the durability of joints. Basically fusion welding is a process combination of rapid heating and cooling cycle. It produces a non-uniform temperature distribution and it causes rapid thermal expansion followed by thermal contraction which in turn develops non-homogeneous plastic deformation and thermal stresses in weldments when it cools down. Cooling rate determines the strength of the weld joint and to make it suitable for structural applications. The thermal cycle appeared in fusion boundary influences the Heat Affected Zone (HAZ) [1]. The thermal conductivity is one of the major thermophysical parameter, need to be evaluated in connection with cooling rate. Also hardness of weldment (at different regions like HAZ, intermediate zone, base metal) shows variation due to the change in cooling rate. There is a continuous effort of welding engineers to control thermal cycle for designing sound and quality joint. Rosenthal [2] laid foundation by developing a steady state analytical model for temperature distribution as well as cooling rate along the fusion boundary. Now it is used for standard comparison due to the involvement of several welding parameters. Quigley [3] demonstrated heat flow from the workpiece of a Tungsten Inert Gas (TIG) welding arc and described cooling mechanism with the help of vaporization and radiation. Svensson [4] presented the experimental and analytical study of cooling curves along the fusion boundary of steel weld deposits. Little and Kamtekar [5] studied the effect of thermal properties in welding efficiency during transient temperature and described the influence of cooling rate. Some recent notable work represented by the researchers such as Komanduri and Hou [6] prescribed analytical and numerical model to develop the expression of cooling rate by using the popular Carslaw and Jaeger's mathematical model. A thorough study on estimation of cooling rate in welding of plates with intermediate thickness accounting heat loss factor has been carried out by Poorhaydari [7]. Gary [8] used Goldak's double ellipsoidal model to find out the effect of welding speed, energy input and heat source distribution on the temperature variation. Arora [9] proposed a generalized correlation developed by dimensional analysis based on theory of rapid solidification. Onsoien [10] performed experimental and simulation study to find out the residual stress affected by cooling rate and evaluated other metallurgical properties based on  $\sigma$ -T curve. Zhang [11] estimated the cooling rate of a spot welded stainless steel nugget based on rapid solidification theory. An analysis of thermal cycle during multipass arc welding has been investigated by Pathak [12] and

simulated cooling rate has been compared with experimental results. Lu [13] carried out to study the cooling rate in high efficient TIG welded Cr13Ni5Mo martensitic stainless steel in connection with surface tension and compared the results with MAG welding joints of same material. Schempp [14] analyzed the microstructure of Al alloys of Gas Tungsten Arc (GTAW) welding bead on plate welding with the variation provided as cooling rate based on cooling rate, thermal gradient and solidification growth rate. Manikandan [15] calculated cooling curves of Inconel 718 fusion zone using argon and helium gas shielded GTAW with a filler metal. Yadaiah and Bag [16] developed heat source model on the basis of 'Egg-shaped' distribution and studied cooling cycles based on numerical as well as experimental results. Motivated by the research work reported as summarized above present analysis has been carried out to estimate cooling curves developed in GTA welding of high carbon steel specimen of grade AISI 1090. Adams empirical correlation has been utilized to develop rate of cooling based on temperatures at predefined locations for a particular time and expression of cooling rate has been derived on the basis of 'Thick Plate model'. Temperatures at different locations along longitudinal direction from fusion boundary has been estimated by inserting thermocouples on the along with Data Acquisition System (DAQ). Thermal conductivity has major influence on cooling rate and the variation has been analyzed based on Carslaw-Jaeger's mathematical model of moving point heat source. As the rate of cooling is much dependent on heat loss in fusion boundary, convection, radiation and evaporation heat loss has been determined and it is compared with well established Vinokurov's heat transfer coefficient due to its coupled radiation-convection characteristics.

## 2. MATHEMATICAL MODELS AND THEORETICAL STUDY

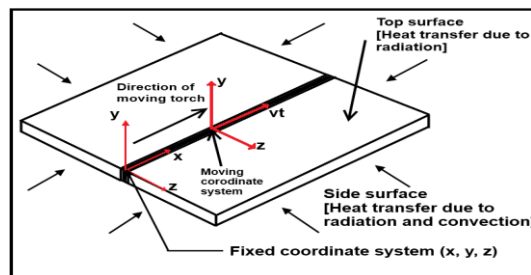


Fig-1. Schematic diagram for moving point heat source in GTA welding

As expressed in fig. 1, the rate of cooling along the z direction from fusion boundary has been analyzed by implementing 'Thick Plate Model' [7]. The temperature distribution based on thick plate model can be mathematically expressed as follows:

$$T - T_0 = \frac{H_{net}}{2\pi kt} \exp\left[-\frac{r^2}{4at}\right] \quad (1)$$

Equation (1) denotes that temperature distribution is function of both time and space. Differentiating equation (1), we have got:

$$\frac{dT}{dt} = -\frac{H_{net}}{2\pi kt^2} \exp\left[-\frac{r^2}{4at}\right] \cdot \left(\frac{r^2}{4at^2}\right) \quad (2)$$

To validate the cooling rate based on equation (2), empirical correlation of cooling rate denoted as Adams cooling rate for 2-dimensional heat flow has been considered and it can be written as [17]:

$$\frac{dT}{dt} = 2\pi k\rho C_p \left(\frac{d}{H_{net}}\right)^2 (T_P - T_0)^3 \quad (3)$$

Theoretically depending upon the thermophysical properties peak temperature at different locations has been estimated by incorporating 'Peak temperature model' [18], and it can be defined mathematically as:

$$\frac{1}{T_P - T_0} = \frac{4.13\rho C_p d.Y}{H_{net}} + \frac{1}{T_m - T_0} \quad (4)$$

Determination of thermal conductivity is important due to its strong influence on cooling rate at different specified locations. By using experimental temperatures cycle data acquired from data acquisition system, the variation of thermal conductivity has been predicted by Carslaw-Jaeger's mathematical model for moving point heat source and mathematically it yields [19]:

$$\theta = \frac{Q_{pt}}{4\pi kR} \exp\left[-\frac{v}{2\alpha}(x + R)\right] \quad (5)$$

The convective heat loss can be formulated as [11]:

$$Q_{conv} = A_{surface} h_c [T_P - T_0] \quad (6)$$

The Radiation heat loss can be expressed as [11]:

$$Q_{rad} = A_{surface} \epsilon\sigma [T_P^4 - T_0^4] \quad (7)$$

The evaporation heat loss can be mentioned as [3]:

$$Q_{evap} = A_{Surface} \omega H_v \quad (8)$$

Where,  $\omega$  is rate of vaporization ( $\text{kg}\cdot\text{s}^{-1}\cdot\text{m}^{-2}$ ) and  $H_v$  is heat of vaporization ( $\text{kJ}/\text{kg}$ ) The mathematical expression for rate of vaporization is given as [3]:

$$\omega = \exp\left[A - \frac{B}{T} - 0.5\ln(T) + C\right] \quad (9)$$

In equation (9), A, B and C are empirical coefficients and T is temperature at particular point of interest. In this paper a technique has been suggested to determine the total heat loss at different locations and mathematically it can be as follows:

$$Q_{\text{Total}} = A_{\text{Surface}} [h_c(T_P - T_0) + \epsilon\sigma(T_P^4 - T_0^4) + \omega H_v] \quad (10)$$

For validation of equation (8), Vinokurov's empirical model [20] of combined convective-radiation heat transfer coefficient (conjugate heat transfer) has been utilized as:

$$h_{\text{vino}} = 2.41 \times 10^{-3} \epsilon T^{1.61} \quad (11)$$

The rate of heat loss based on equation (9) can be given as:

$$Q'_{\text{Total}} = A_{\text{Surface}} h_{\text{vino}} (T_P - T_0) \quad (12)$$

### 3. EXPERIMENTATION

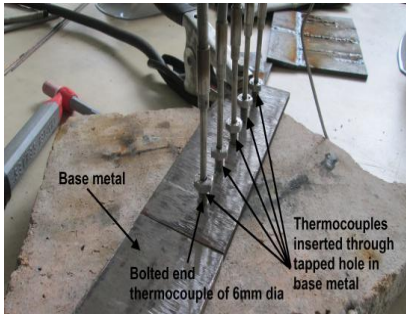


Fig-2. Five thermocouples inserted through tapped hole in plate

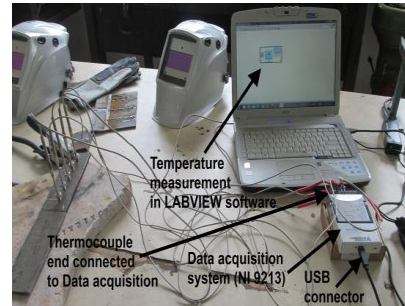


Fig-3. Connection of thermocouples with Data acquisition system and computer

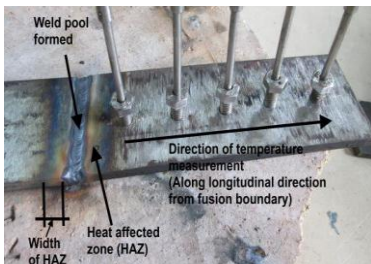


Fig-4. Weld pool formed after single pass welding



Fig-5. Broad view of heat affected zone developed in joint

Experimental work has been carried out to predict the temperature cycle developed in weld joint. Five thermocouples have been inserted on the surface of the plate maintaining 30mm distance between each, along the longitudinal direction from the fusion boundary (refer fig. 1).

**Table-1.** Chemical composition of AISI 1090 [21, 22]

Element:	C	Fe	Mn	P	S
Percentage (%):	0.85 - 0.98	98.03 - 98.55	0.60 - 0.90	0.040	0.050

**Table-2.** Details of instruments used for experiment

Specimen	<b>Material: AISI 1090</b> <b>Dimension: 180×60×10mm</b>
GTAW System	Welding amperage range: 3–350A, Rated output: 250A at 30V, 100% Duty cycle, Maximum open circuit voltage: 75VDC
Data Acquisition System (DAQ)	NI 9213, 16 Channel, 24bit thermocouple, CAT II, Ch. To earth insulation
Filler metal	Copper coated triple de-oxidized mild steel rod
Inert gas used	Argon
Thermocouple	K type

The tapped holes has been made on the surface of the plate to insert the thermocouple end. Table 1 denotes the experimental apparatus used for measurement. The rear end of the thermocouple has been connected to the Data acquisition system to acquire the temperature at different locations for a fixed interval of time and it has simulated in LABVIEW software (refer fig. 2). The weld bead formed by GTAW and corresponding HAZ can be visualized in fig. 5. The experimental process parameters and thermophysical properties of AISI 1090 are tabulated in table 3 and table 4 respectively.

**Table-3.** Thermophysical properties of AISI 1090 (at 30°C) [21]

Density (kg/m <sup>3</sup> )	7790
Specific heat (J/kg-°C)	0.465
Thermal conductivity (w/m-°C)	49.8
Thermal diffusivity (m <sup>2</sup> /s)	13.74

**Table-4.** Experimental process parameters

Input current (A)	150
Input voltage (V)	12.8
Time of completing single pass(s)	70
Electrode speed (mm/s)	0.857
Heat input (w)	1632
Heat transfer efficiency (%)	85
Radius of GTAW flux (mm)	3
Surface area (mm <sup>2</sup> )	10800
Heat transfer coefficient (w/m <sup>2</sup> -K)	10
Stefan Boltzmann constant (J/m <sup>2</sup> -K <sup>4</sup> )	$5.67 \times 10^{-8}$
Emissivity	0.8

The weld bead formed by GTAW and corresponding HAZ can be visualized in fig. 4. The experimental process parameters and thermophysical properties of AISI 1090 are tabulated in table 3 and table 4 respectively.

#### 4. RESULTS AND DISCUSSION

Fig. 6 depicts the temperature cycle produced during the time of formation of weld bead measures along the longitudinal direction from fusion boundary (refer fig. 4). It is clear from fig. 6 that temperature attained maximum through time interval in the region of  $z = 36\text{mm}$  and  $z = 72\text{mm}$ . As  $z = 36\text{mm}$  and  $z = 72\text{mm}$  are very near to the heat affected zone (HAZ) and the intermolecular energy exchange near the fusion line is in rapid manner. So the locations as denoted  $z = 108, 144$  and  $180\text{mm}$  from fusion boundary are not effected as compared to  $z = 36\text{mm}$  and  $z = 72\text{mm}$ . Also from fig. 6 it can be easily predicted that heating cycle is very fast compared to cooling cycle, though there are some sudden drop in temperatures at  $z = 36, 72, 108\text{mm}$  but after  $600^\circ\text{C}$  the slope of curves are very less in cooling cycle as compared with heating cycle. The sudden rise and drop of temperature defines the transient nature of thermal cycle developed. Fig. 7 denotes the theoretical study of analyzing peak temperatures at different predefined locations on the basis of peak temperature model as expresses in equation (4). Fig. 7 reveals the steady state temperature cycle due to the constant thermophysical properties (refer table 3) of AISI 1090. This results (both fig. 6 and fig. 7) shows good agreement with the work analyzed by Pathak [12].

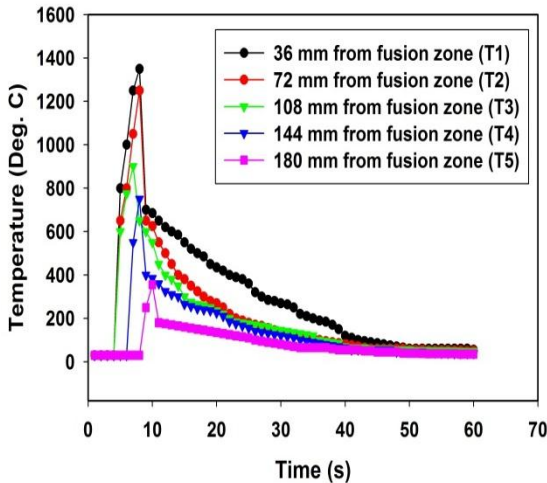


Fig-6. Experimental temperature distribution from fusion boundary to longitudinal direction with time

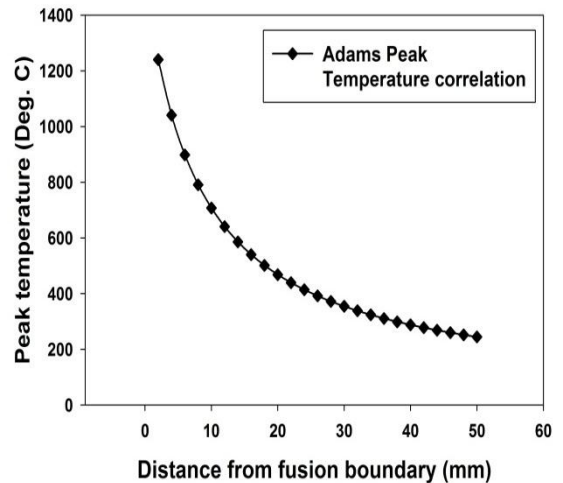


Fig-7. Theoretical peak temperature distribution from fusion boundary to longitudinal direction with space

Figure 8 represents the estimation of temperature variation based on theoretical thermal conductivity of AISI 1090 of different temperatures along the longitudinal direction from fusion line. Thermal conductivity measures the propagation of heat from the material and as well as it influences the cooling rate of the material.

According to Carslaw-Jaegers’s moving point heat source model (refer equation 5), it has been justified that for higher thermal conductivity temperature is high whereas for lower thermal conductivity, temperature has attained maximum value (based on Fourier’s law of heat conduction). Figure 9 shows the variation of thermal conductivity with respect to time calculated on the basis of Carslaw-Jaeger’s mathematical model by using experimental temperatures different location on particular interval of time. At  $z = 36\text{mm}$  thermal conductivity is initially very high as the higher temperature attained after 5s and sudden drop in thermal conductivity shows the attenuation of maximum temperature after 5s which can be justified by fig. 6. The variation reveals the transient nature of thermal conductivity and rapid change in the property on high temperatures for a very small period of time. In the work reported by Komanduri and Hou [6], they have determined the variation of temperature rise for mild steel arc welded joints and fig. 8 directly matches with the results on the basis of high carbon steel joints in present work.

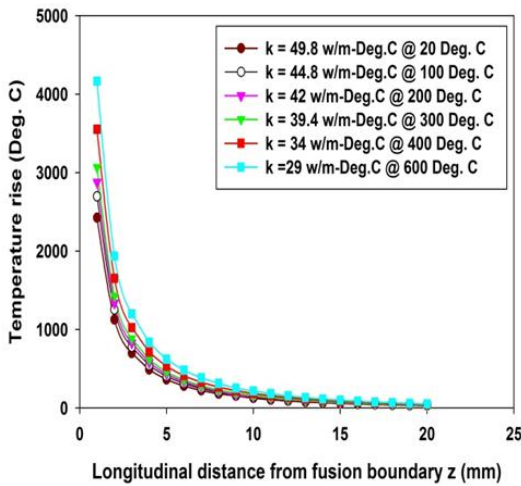


Fig-8. Variation of temperature rise towards longitudinal direction from fusion boundary for different values of thermal conductivity

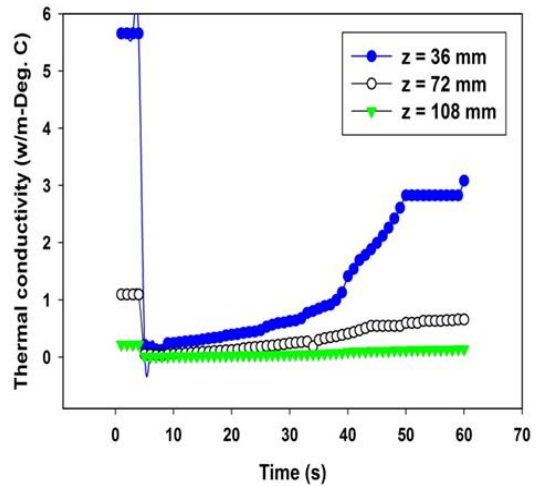


Fig-9. Variation of thermal conductivity at different locations due to temperature rise with time period

Figure 10 has specified the rate of cooling at predefined locations (experimental temperature data) defined on the basis of Adams model (refer equation 3). The nature of cooling rate itself justifies the nature of thermal cycle produced during formation of weld pool. Also it can be said that in the period of 150s measurement of temperature, cooling cycle rapidly changes only during first 5-10s. The heat loss due to coupled convection and radiation is very fast near the HAZ. After  $z = 72\text{mm}$  there is no rapid changes in cooling rate takes place as the locations are far from fusion boundary. This results can be easily compared with negligible variation with the results developed by Gary [8].

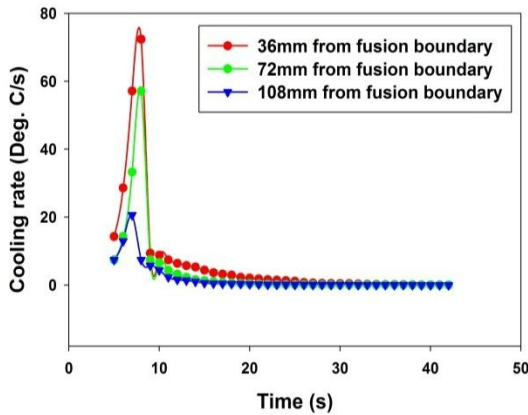


Fig-10. Rate of cooling with respect to time at different specified locations based on Adams correlation

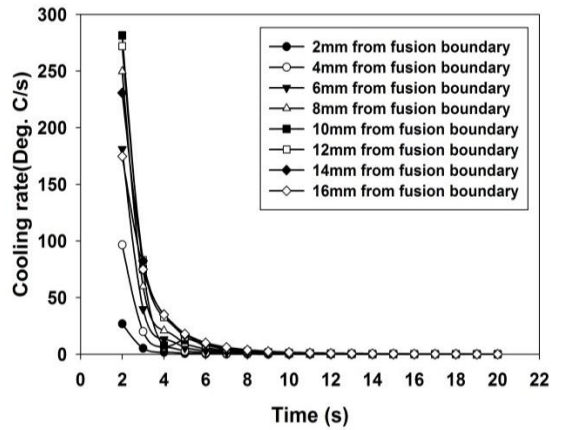


Fig-11. Rate of cooling with respect to time based along longitudinal direction based on Thick Plate model

Cooling rate based on Thick plate model as derived in equation (2), is presented in fig. 11. As this expression does not include the temperature term and instead of that it is consisting of time and space, analysis has been carried out to find the change in cooling rate at very minute positions from fusion line. At location  $z = 2\text{mm}$  from fusion boundary the cooling rate is less as the heat propagation is less at initial times and it is continued for  $z = 6\text{mm}$ . After attaining the heating cycle (refer fig. 6), at  $z = 8\text{mm}$  to  $z = 10\text{mm}$ , cooling rate is maximum due to rapid temperature increment and after that  $z = 12\text{mm}$  to  $z = 16\text{mm}$  rate of cooling decreases due to gradual temperature fall. Thus cooling rate in fig. 11 can be easily compared with the empirical correlation of Adams model. Also fig. 10 and fig. 11 shows well agreement with the work represented by Little and Kamtekar [5] and Komanduri and Hou [6].

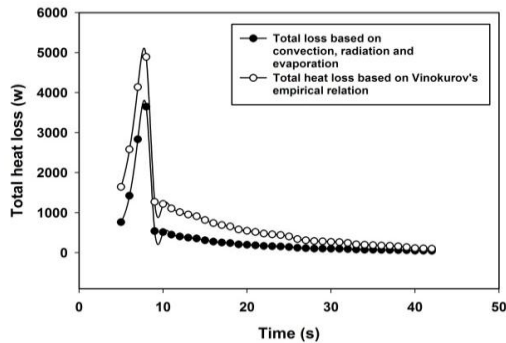


Fig-12. Variation of heat loss with respect to time based on proposed correlation and Viokurov's empirical correlation at  $z = 36\text{mm}$  from fusion boundary

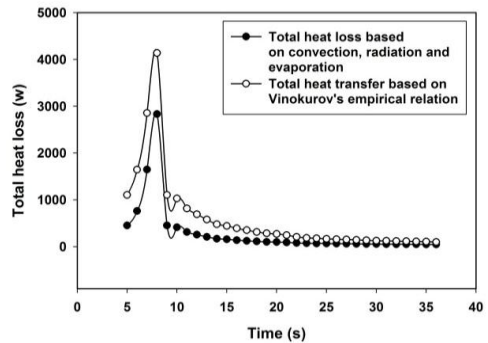


Fig-13. Variation of heat loss with respect to time based on proposed correlation and Viokurov's empirical correlation at  $z = 72\text{mm}$  from fusion boundary

In present investigation a method has been suggested to find out the total heat transfer based on experimental temperature data. Equation 10 is indicating the total heat loss as proposed by summation of conduction, radiation and evaporation heat loss. Though there is very little contribution of evaporation heat transfer in welding phenomena, but still it has been considered

due to formation of melting steel at highest temperature in the weld pool for a fraction of second. At higher temperatures ( $>800^{\circ}\text{C}$ ) from the calculation on the basis of equation (6) and equation (7), it has found out that radiation heat transfer has major influence than convective heat transfer. As near the fusion boundary the inter-molecular energy exchange is maximum compared to other regions in welded joints. Also the moving GTA torch provides flame (along with argon gas) and direct current electrode negative. (DCEN) combination has used for generating electric arc. This signifies the possibility of radiation heat transfer. Whereas in the rear end of the plates (region far from fusion line) has lower temperatures due to heat loss and convection dominates the radiation at lower temperatures ( $<750^{\circ}\text{C}$ ). The reason is heat exchange of surrounding air with the plates end. Both fig. 12 and fig. 13 have indicated that heat loss is maximum in the time range between 5s - 10s. Proposed technique has been easily compared with the established Vinokurov's empirical correlation due to same nature and it also justifies the experimental thermal cycle (refer fig. 6). Due to involvement of constant term in Vinokurov's empirical correlation, magnitude of heat loss is greater than proposed relation. With the research paper presented by Pathak [12] and Lu [13] present analysis of heat loss from weld joints can be well predicted.

## 5. CONCLUSION

From the current research investigation the following remarks can be concluded:

- Experimental temperature cycle for GTA welding of high carbon steel is maximum near the heat affected zone ( $z = 36\text{mm}$  and  $z = 72\text{mm}$ ). At same time interval other locations ( $z = 108, 144, 180\text{mm}$ ) maximum temperature attained is very less due to rapid heat loss in movement of GTA torch.
- At  $z = 36\text{mm}$ , a vigorous decrement of thermal conductivity (from  $5.655\text{ w/m-deg. C}$  to  $0.125\text{ w/m-deg}$ ) has been observed due to formation of transient temperature field and it also reveals the suitability of application of Carslaw-Jaeger's mathematical model for moving point heat source.
- Rate of cooling analyzed both on the basis of 'Thick Plate Model' and 'Adams 2D correlation' has justified the experimental thermal cycle and show a significant cooling rate near the HAZ.
- The major influential property in connection with cooling rate, is heat loss and it justifies the rate of cooling. Proposed method of cooling rate has been well judged by established correlation as well as experimental thermal cycle.

## REFERENCES

- [1] J. A. Goldak and M. Akhlaghi, *Computational welding mechanics*. Springer Street, New York 100013, USA: Springer Science+Business Media Inc, 2005.
- [2] D. Rosenthal, "The theory of moving sources of heat and its applications in metal treatments," *Trans. ASME.*, vol. 68, pp. 849 -865, 1946.

- [3] M. B. C. Quigley, "Heat flow to the workpiece from a TIG welding arc," *J. Phys. D:Appl. Phys.*, vol. 6, pp. 2250-2258, 1973.
- [4] L. E. Svensson, "An analysis of cooling curves from the fusion zone of steel weld deposits," *Sc. and J. Metallurgy*, vol. 15, pp. 97-103, 1986.
- [5] G. H. Little and A. G. Kamtekar, "The effect of thermal properties and weld efficiency on transient temperatures in welding," *Computers and Structures*, vol. 68, pp. 157 -165, 1998.
- [6] R. Komanduri and Z. B. Hou, "Thermal analysis of arc welding process: Part II. Effect of thermophysical properties with temperature," *Metallurgical and Materials Transactions B*, vol. 33B, pp. 483 - 499, 2001.
- [7] K. Poorhaydari, "Estimation of cooling rate in the welding of plates with intermediate thickness," *Welding Journal*, vol. 84, pp. 149s-155s, 2005.
- [8] D. Gary, "Effect of welding speed, energy input and heat source distribution on temperature variations in butt welding," *Journal of Material Processing Technology*, vol. 167, pp. 393 - 401, 2005.
- [9] A. Arora, "Cooling rate in 800 to 500°C range from dimensional analysis," *Science and Technology of Welding and Joining*, vol. 15, pp. 423-427, 2010.
- [10] M. I. Onsoien, "Residual stresses in weld thermal cycle simulated specimens of X70 pipeline steel," *Welding Journal*, vol. 89, pp. 127-132, 2010.
- [11] Y. Zhang, "Estimating of cooling rates of spot welding nugget in stainless steel," *Welding Journal*, vol. 91, pp. 247-251, 2012.
- [12] C. S. Pathak, "Analysis of thermal cycle multipass arc welding," *Welding Journal*, vol. 91, pp. 149s -155s, 2012.
- [13] S. P. Lu, "Highly efficient TIG welding of Cr13Ni5Mo martensitic stainless steel," *Journal of Material Processing Technology*, vol. 213, pp. 229 - 237, 2013.
- [14] P. Schempp, "Solidification of GTA aluminum weld metal: Part 2 — thermal conditions and model for columnar-to-equiaxed transition," *Welding Journal*, vol. 93, pp. 69-77, 2014.
- [15] S. G. K. Manikandan, "Effect of weld cooling rate on laves phase formation in inconel 718 fusion zone," *Journal of Material Processing Technology*, vol. 214, pp. 358-364, 2014.
- [16] N. Yadaiah and S. Bag, "Development of egg-configuration heat source model in numerical simulation of autogenous fusion welding process," *International Journal of Thermal Sciences*, vol. 86, pp. 125-138, 2014.
- [17] S. Kou, *Welding metallurgy. Willey-interscience, 111 river street*, 2nd ed. Hoboken, New Jersey 07030: A John Willey and Sons Inc. Publication, 2003.
- [18] N. R. Mandal, *Welding and distortion control*, 1st ed. New Delhi: Narosa Publishing House, Darya Ganj, Delhi Medical Association Road, 2004.
- [19] H. S. Carslaw and J. S. Jaeger, *Conduction of heat in solids*, 2nd ed. Oxford, United Kingdom: Oxford University Press, 1959.
- [20] R. S. Desai and S. Bag, "Influence of displacement constraints in thermomechanical analysis of laser micro-spot welding process," *Journal of Manufacturing Process*, vol. 16, pp. 164 - 275, 2014.
- [21] G. E. Dieter, *Mechanical metallurgy*, 3rd ed.: McGraw Hill Education Pvt. Ltd.
- [22] ASM Handbook, "Welding, brazing and soldering," *ASM International*, vol. 6, 1993.

## NOMENCLATURE

<b>x</b>	<b>Space coordinate along fusion boundary (mm)</b>
<b>z</b>	Space coordinate along longitudinal direction from fusion boundary
<b>T</b>	Temperature at specific location ( $^{\circ}\text{C}$ )
<b>T<sub>0</sub></b>	Ambient temperature ( $^{\circ}\text{C}$ )
<b>r</b>	Radial distance from fixed coordinate (mm)
<b>v</b>	Welding velocity (mm/s)
<b>T<sub>p</sub></b>	Peak temperature ( $^{\circ}\text{C}$ )
<b>k</b>	Thermal conductivity (w/m $^{\circ}\text{C}$ )
<b><math>\alpha</math></b>	Thermal diffusivity (m $^2$ /s)
<b>C<sub>p</sub></b>	Specific heat (J/kg- $^{\circ}\text{C}$ )
<b>h<sub>c</sub></b>	Convective heat transfer coefficient (w/m $^2$ - $^{\circ}\text{C}$ )
<b><math>\epsilon</math></b>	Emissivity
<b><math>\sigma</math></b>	Stefan-Boltzmann constant (J/m $^2$ -K $^4$ )
<b>I</b>	Current (A)
<b>V</b>	Voltage (v)
<b><math>\eta</math></b>	Heat transfer efficiency (%)
<b><math>\omega</math></b>	Vaporization rate (kg/s-m $^2$ )
<b>H<sub>v</sub></b>	Heat of vaporization (J/kg)
<b>h<sub>vino</sub></b>	Vinokurov's heat transfer coefficient (w/m $^2$ - $^{\circ}\text{C}$ )
<b>A<sub>Surface</sub></b>	Surface area (mm $^2$ )
<b>d</b>	Plate thickness (mm)
<b>t</b>	Time (s)
<b>T<sub>m</sub></b>	Melting point temperature ( $^{\circ}\text{C}$ )
<b><math>\rho</math></b>	Density (kg/m $^3$ )
Subscripts	rad: Radiation conv: Convection evap: Evaporation Vino: Vinokurov's empirical correlation

*Views and opinions expressed in this article are the views and opinions of the author(s), Review of Industrial Engineering Letters shall not be responsible or answerable for any loss, damage or liability etc. caused in relation to/arising out of the use of the content.*